Acta Crystallographica Section F
Structural Biology and Crystallization Communications
ISSN 1744-3091

Structure of the stand-alone RAM-domain protein from *Thermus thermophilus* HB8

Noboru Nakano,[a]‡ Nobuo Okazaki,[a]‡ Shinya Satoh,[a] Koji Takio,[a] Seiki Kuramitsu,[a,b] Akeo Shinkai[a] and Shigeyuki Yokoyama[a,c,d]*

[a]RIKEN SPring-8 Center, Harima Institute, 1-1-1 Kouto, Sayo, Hyogo 679-5148, Japan, [b]Department of Biology, Graduate School of Science, Osaka University, Toyonaka, Osaka 560-0043, Japan, [c]RIKEN Genomic Sciences Center, 1-7-22 Suehiro-cho, Tsurumi, Yokohama 230-0045, Japan, and [d]Department of Biophysics and Biochemistry, Graduate School of Science, University of Tokyo, 7-3-1 Hongo, Bunkyo-ku, Tokyo 113-0033, Japan

‡ These authors contributed equally to this work.

Correspondence e-mail: yokoyama@biochem.s.u-tokyo.ac.jp

Received 6 July 2006
Accepted 8 August 2006

PDB Reference: TTHA0845, 2djw, r2djwsf.

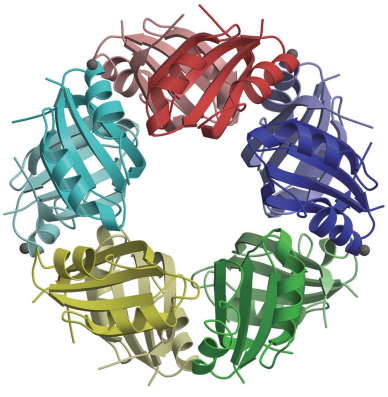

The stand-alone RAM (regulation of amino-acid metabolism) domain protein SraA from *Thermus thermophilus* HB8 (TTHA0845) was crystallized in the presence of zinc ions. The X-ray crystal structure was determined using a multiple-wavelength anomalous dispersion technique and was refined at 2.4 Å resolution to a final *R* factor of 25.0%. The monomeric structure is a $\beta\alpha\beta\beta\alpha\beta$ fold and it dimerizes mainly through interactions between the antiparallel β-sheets. Furthermore, five SraA dimers form a ring with external and internal diameters of 70 and 20 Å, respectively. This decameric structure is unique compared with the octameric and dodecameric structures found for other stand-alone RAM-domain proteins and the C-terminal RAM domains of Lrp/AsnC-family proteins.

1. Introduction

The Lrp/AsnC-family transcriptional regulators (Calvo & Matthews, 1994), also termed feast/famine regulatory proteins (FFRPs; Suzuki, 2003), are widely distributed in bacteria and archaea (Brinkman *et al.*, 2003). The *Escherichia coli* leucine-responsive regulatory protein (Lrp), which is the most studied member of this family, is a global regulator that controls a large number of genes and operons, including those involved in amino-acid metabolism, either positively or negatively (Calvo & Matthews, 1994; Newman & Lin, 1995). In these regulons, Lrp activity is modulated by leucine, which is the major effector. In archaea, the properties of several Lrp-like regulators have been characterized (Bell & Jackson, 2001; Ouhammouch, 2004; Geiduschek & Ouhammouch, 2005).

The crystal structures of various Lrp/AsnC-family proteins, such as *Pyrococcus furiosus* LrpA, *Pyrococcus* sp. FL11, *E. coli* AsnC and *Bacillus subtilis* LrpC, have been determined (Leonard *et al.*, 2001; Koike *et al.*, 2004: Thaw *et al.*, 2006). The proteins consist of an N-terminal helix–turn–helix DNA-binding domain connected by a hinge to the C-terminal RAM (regulation of amino-acid metabolism) domain, with a $\beta\alpha\beta\beta\alpha\beta$ fold. This fold is strikingly similar to that of the ACT (aspartokinase, chorismate mutase and TyrA) domain, a ubiquitous allosteric regulatory domain within many metabolic enzymes; the ACT domain of *E. coli* D-3-phosphoglycerate dehydrogenase (PGDH), for example, binds the effector molecule L-serine (Ettema *et al.*, 2002; Schuller *et al.*, 1995). The Lrp/AsnC-family proteins form symmetric dimers, mainly through interactions between the antiparallel β-sheets of the C-terminal RAM domain. The LrpA, AsnC and LrpC structures revealed four dimers are arranged as a disc, with their RAM domains contacting in the centre and their N-terminal domains facing outward (Leonard *et al.*, 2001; Thaw *et al.*, 2006). In the case of the FL11 protein, the dimers form a sixfold helix, also with the RAM domains facing toward the centre and the N-terminal domains facing outward (Koike *et al.*, 2004). The RAM domain of the Lrp/AsnC-family proteins may be involved in their effector-dependent allosteric regulation (Brinkman *et al.*, 2003). In fact, bound asparagine molecules were found in the RAM domain of *E. coli* AsnC (Thaw *et al.*, 2006).

Table 1
Summary of crystal parameters, data-collection and refinement statistics.

Values in parentheses are for the highest resolution shells.

	Native	Peak	Edge	Remote
Wavelength (Å)	1.0000	1.2822	1.2828	1.2600
Space group	$P3_2$	$P3_2$		
Unit-cell parameters (Å, °)	$a = b = 95.883$, $c = 119.010$, $\gamma = 120$	$a = b = 95.374$, $c = 118.413$, $\gamma = 120$		
Resolution (Å)	2.4 (2.49–2.4)	2.5 (2.59–2.5)	2.7 (2.80–2.70)	2.6 (2.69–2.6)
No. of measured reflections	299648	243415	206851	229908
No. of unique reflections	47780	41345	33077	37018
R_{merge}† (%)	4.0 (30.4)	5.7 (22.8)	4.6 (13.3)	4.6 (17.1)
Data completeness (%)	99.9 (100)	99.3 (93.6)	99.9 (100)	100 (100)
$I/\sigma(I)$ (%)	17.6 (6.8)	15.9 (5.9)	20.3 (11.9)	19.1 (9.3)
R factor‡ (%)	25.0			
R_{free} (%)	29.4			
No. of protein atoms	6229			
No. of water molecules	226			
R.m.s.d. bonds (Å)	0.012			
R.m.s.d. angles (°)	1.394			

† $R_{merge} = \sum |I - \langle I \rangle| / \sum I$. ‡ R factor and $R_{free} = \sum ||F_o| - |F_c|| / \sum F_o|$, where the free reflections (5% of total used) were reserved for R_{free} throughout refinement.

Archaea and bacteria also have proteins bearing the RAM domain, but lacking the DNA-binding domain. These are classified as stand-alone RAM-domain (SARD) proteins (Ettema *et al.*, 2002), which are also called headless Lrp/AsnC proteins (Kudo *et al.*, 2001) and demi-FFRPs (Koike *et al.*, 2003), and their role has not yet been elucidated. It has been speculated that their function might be similar to that of *E. coli* IlvH, which is the ACT-containing small regulatory subunit of acetohydroxyacid synthase isozyme III (Mendel *et al.*, 2001). The IlvH subunit associates with the catalytic subunit IlvI and is responsible for the full activity and the valine-inhibition of the holoenzyme. The SARD proteins may also have some function by themselves, as the *P. furiosus* SARD protein Q8U228 displays hydrolytic activity against chromogenic esters (Agapay *et al.*, 2005). Two SARD proteins, *Pyrococcus* sp. DM1 and *P. furiosus* Q8U228, have been crystallized (Kudo *et al.*, 2001; Agapay *et al.*, 2005). The DM1 structure is similar to that of the C-terminal RAM domains of LrpA, LrpC and AsnC, with the four dimers arranged in a ring (Koike *et al.*, 2003). In solution, DM1 adopts different oligomeric states depending on the presence or absence of effector molecules such as hydrophobic amino acids and some metabolic intermediates (Sakuma *et al.*, 2005). Yokoyama *et al.* (2006) reported that DM1 can be heterologously assembled with the full-length Lrp/AsnC protein. Based on these observations, it was proposed that DM1 functions in transcriptional regulation by Lrp/AsnC-family proteins.

Here, we describe the crystal structure of the SARD protein SraA from *Thermus thermophilus* HB8 (TTHA0845), which shares 25.0% identity and 46.7% similarity in its amino-acid sequence to that of DM1.

2. Materials and methods

2.1. Protein preparation and gel-filtration analysis

The *SraA* gene (TTHA0845) was amplified by PCR using *T. thermophilus* HB8 genomic DNA as the template. The amplified fragment was cloned under the control of the T7 promoter of the *E. coli* expression vector pET-11a (Novagen, Madison, WI, USA). The expression vector was introduced into the *E. coli* BL21 (DE3) strain (Novagen) and the recombinant strain was cultured in 6 l LB medium supplemented with 50 µg ml^{-1} ampicillin. The cells (22.1 g) were collected by centrifugation, washed with buffer *A* (20 m*M* Tris–HCl buffer pH 8.0) containing 50 m*M* NaCl and resuspended in the same buffer. The cells were then disrupted by sonication in a chilled water bath and the cell lysate was incubated at 343 K for 10 min. Ammonium sulfate was added to the supernatant to a final concentration of 1.5 *M* and the protein was collected as a precipitate. The pellet was dissolved in buffer *A* and desalted by fractionation on a HiPrep 26/10 desalting column (Amersham Biosciences, Uppsala, Sweden). The sample was applied onto a Resource Q column (Amersham Biosciences) pre-equilibrated with buffer *A*, which was eluted with a linear gradient of 0–1 *M* NaCl. The eluted fractions containing the recombinant SraA protein were applied onto a HiTrap heparin column (Amersham Biosciences) pre-equilibrated with 20 m*M* MES buffer pH 6.0, which was eluted with a linear gradient of 0–1 *M* NaCl. The eluted fractions containing the SraA protein were pooled and then applied onto a hydroxyapatite CHT10 column (Bio-Rad Laboratories Inc., Hercules, CA, USA), which was eluted with a linear gradient elution of 10–500 m*M* sodium phosphate buffer pH 7.0. The sample containing the SraA protein was then loaded onto a Mono Q column (Amersham Biosciences) pre-equilibrated with buffer *A*, which was eluted with a linear gradient of 0–0.5 *M* NaCl. The fractions containing the SraA protein were collected and then applied onto a HiLoad 16/60 Superdex 75pg column (Amersham Biosciences) pre-equilibrated with buffer *A* containing 150 m*M* NaCl. The purified SraA protein was loaded on a HiPrep 26/10 desalting column, which was eluted with buffer *A* containing 1 m*M* dithiothreitol (DTT). The SraA protein was concentrated with a Vivaspin 20 concentrator (5 kDa molecular-weight cutoff, Sartorius, AG, Goettingen, Germany). The protein concentration was determined by measuring the absorbance at 280 nm (Kuramitsu *et al.*, 1990).

SDS–PAGE was performed with pre-cast 5–20%(*w*/*w*) polyacrylamide gels (ATTO Corp., Tokyo, Japan) according to the method of Laemmli (1970) and the gels were stained with Coomassie Brilliant Blue R-250.

The SraA protein, mixed with molecular-weight standards, was applied onto a Superdex 200 3.2/30 (Amersham Biosciences) column using HPLC (model 1100, Agilent Technologies, Palo Alto, CA) at a flow rate of 50 µl min^{-1}. Buffer *A* was used as the elution buffer.

2.2. Crystallization

Crystallization of the SraA protein was performed by the sitting-drop vapour-diffusion method. Initial screening was explored using several kits from Hampton Research (Aliso Veijo, CA, USA) and Emerald Biosystems (Bainbridge Island, WA, USA) by mixing 1 µl of 8.35 mg ml^{-1} protein in buffer *A* containing 1 m*M* DTT with an equal volume of the reservoir solution at 293 or 281 K. During the course of screening, crystals with suitable shapes appeared only in conditions containing zinc ions. The size and quality of the crystals were improved by varying the concentration of precipitant, salt, buffer and pH. The best crystals grew to dimensions of 0.2 × 0.2 × 0.2 mm at 281 K in a solution containing 2% PEG 3350, 20 m*M* zinc acetate and 10 m*M* MES pH 6.5.

2.3. X-ray data collection and processing

The crystals thus obtained were washed in 2% PEG 3350, 10 m*M* MES buffer pH 6.5 and were gradually equilibrated in 31% ethylene glycol, 2% PEG 3350 and 10 m*M* MES buffer pH 6.5. The crystals were mounted in a nylon-fibre loop and were then cooled in a nitrogen-gas stream at 100 K. Multiple-wavelength anomalous dispersion (MAD) data sets at 2.5 Å resolution with three different

wavelengths near the absorption edge of zinc and a native data set at 2.4 Å resolution were collected at 100 K using the RIKEN Structural Genomics Beamline II (BL26B2) at SPring-8 (Hyogo, Japan) with a Jupiter 210 CCD detector (Rigaku MSC Co., Tokyo, Japan). The diffraction images were processed using the *HKL*-2000 program package (Otwinowski & Minor, 1997). The two zinc sites were found and refined using the MAD data set and the initial phases were calculated using the programs *SOLVE* (Terwilliger & Berendzen, 1999) and *RESOLVE* (Terwilliger, 2001). Improvement of the phases by solvent flattening and histogram matching and automatic building of a partial model of the protein were performed with the program *ARP/wARP* (Morris *et al.*, 2003).

2.4. Structure refinement and model building

Rigid-body refinement, simulated-annealing torsion-angle refinement and individual *B*-factor refinement were performed with *CNS* v.1.1 (Brünger *et al.*, 1998) and *REFMAC* (Murshudov *et al.*, 1997). Several rounds of refinement combined with model rebuilding and initial picking and manual verification of water molecules were

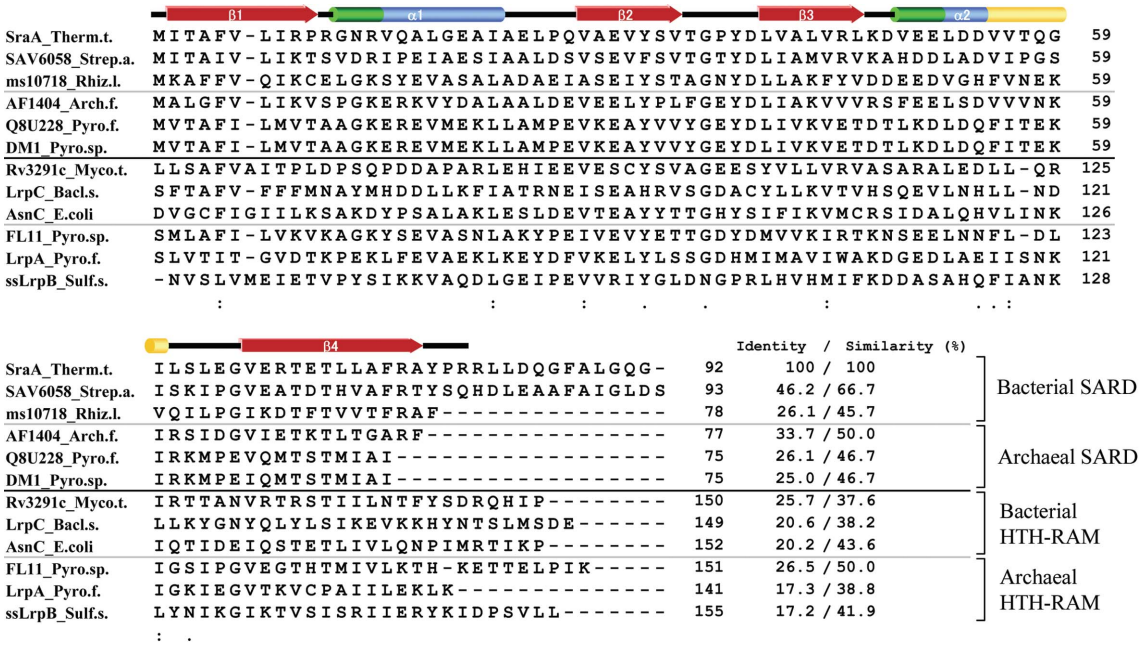

Figure 1
Amino-acid sequence alignment of *T. thermophilus* SraA (TTHA0845) with SARD proteins and C-terminal RAM domains of Lrp/AsnC-family proteins (HTH-RAM). The sequences were aligned using *ClustalW* (Thompson *et al.*, 1994). Secondary-structure elements of SraA, obtained using the *DSSP* program (Kabsch & Sander, 1983), are shown above the alignment. Red, green, blue and yellow represent β-strand, 3_{10}-helix, α-helix and π-helix, respectively. Species abbreviations are as follows: Therm.t., *Thermus thermophilus*; Rhiz.l., *Rhizobium loti*; Strep.a., *Streptomyces avermitilis*; Arch.f., *Archaeoglobus fulgidus*; Pyro.f., *Pyrococcus furiosus*; Pyro.sp., *Pyrococcus* sp.; Myco.t., *Mycobacterium tuberculosis*; Bacl.s., *Bacillus subtilis*; E.coli, *Escherichia coli*; Sulf.s., *Sulfolobus solfataricus*. The amino-acid sequences of the Q8U228_Pyro.f. and DM1_Pyro.sp proteins are the same as those of the *P. furiosus* PF1022 and *P. horikoshii* PHS023 proteins, respectively.

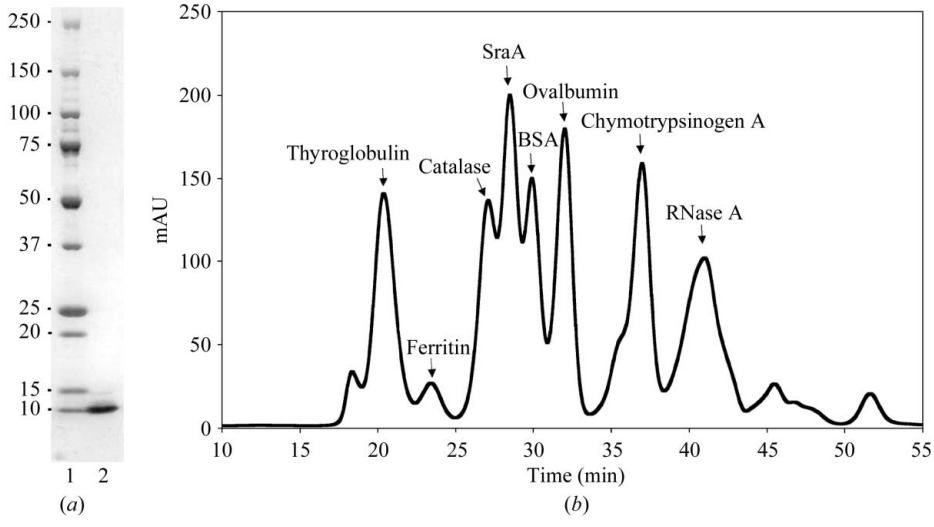

Figure 2
Purification and gel-filtration analysis of the recombinant SraA protein. (*a*) The recombinant protein (3 µg) was analyzed by SDS–PAGE (lane 2). Lane 1, molecular-weight markers (kDa). (*b*) The purified SraA protein (3.36 µg/1.7 µl) was analyzed by gel-filtration column chromatography in the presence of 0.4 µg thyroglobulin (669 kDa), 0.9 µg ferritin (440 kDa), 0.2 µg catalase (158 kDa) and 1.3 µg each of bovine serum albumin (BSA) (67 kDa), ovalbumin (43 kDa), chymotrypsinogen A (20.4 kDa) and RNase A (13.7 kDa). The elution profile of the sample was detected by measuring A_{215}. The peak for each protein is indicated by an arrow.

performed with *Coot* (Emsley & Cowtan, 2004). The geometry of the final structure was checked with *PROCHECK* (Laskowski *et al.*, 1993). The data-collection and refinement statistics are summarized in Table 1.

3. Results and discussion

3.1. Primary structure and purification

The *T. thermophilus* SraA protein is a functionally uncharacterized protein consisting of 92 amino-acid residues, with a predicted molecular weight of 10.1 kDa and a potential pI of 4.52. The amino-acid sequence of the protein shares homology with the SARD proteins and the C-terminal RAM domains of the Lrp/AsnC-family proteins (Fig. 1).

The recombinant SraA protein expressed in *E. coli* cells was purified from the heat-treated cell lysate by ammonium sulfate precipitation followed by heparin, anion-exchange, hydroxyapatite and gel-filtration column chromatography steps. The purified protein (more than 95% purity; Fig. 2*a*) was analyzed by gel filtration to determine the oligomeric state in solution. The retention time of the protein was around 28 min and the apparent molecular weight of the SraA protein was estimated to be around 110 kDa (Fig. 2*b*). These results indicate that the SraA protein forms an oligomer (decamer or undecamer) in solution. Other peaks derived from the SraA protein were hardly detectable (data not shown), in contrast to the results of gel-filtration experiments for the *Pyrococcus* sp. DM1 protein, in which four main peaks, corresponding to hexadecamer/octamer, hexamer, tetramer and dimer, were observed (Sakuma *et al.*, 2005).

3.2. Crystallization, data processing and structure

The SraA protein was crystallized using the sitting-drop vapour-diffusion method. Crystals suitable for structural determination only appeared in conditions containing zinc ions. The crystals were washed and equilibrated with a zinc-free cryoprotectant and were then cooled in a nitrogen-gas stream at 100 K. The structure was determined using the MAD methodology and was refined to 2.4 Å resolution. The final structure was checked with the program *PROCHECK*; the model has 92.2% of the residues in the most favoured conformation of the Ramachandran plot, with 7.8% in the additional allowed region (data not shown).

The structure of the SraA protein consists of two α-helices and a four-stranded antiparallel β-sheet that form a ferredoxin-like $\beta\alpha\beta\beta\alpha\beta$-fold, in which two α-helices, $\alpha1$ and $\alpha2$, are packed on one side (Fig. 3*a*).

The monomer forms a dimer related by a non-crystallographic twofold axis (Fig. 3*a*). The dimer is mainly composed of hydrophobic

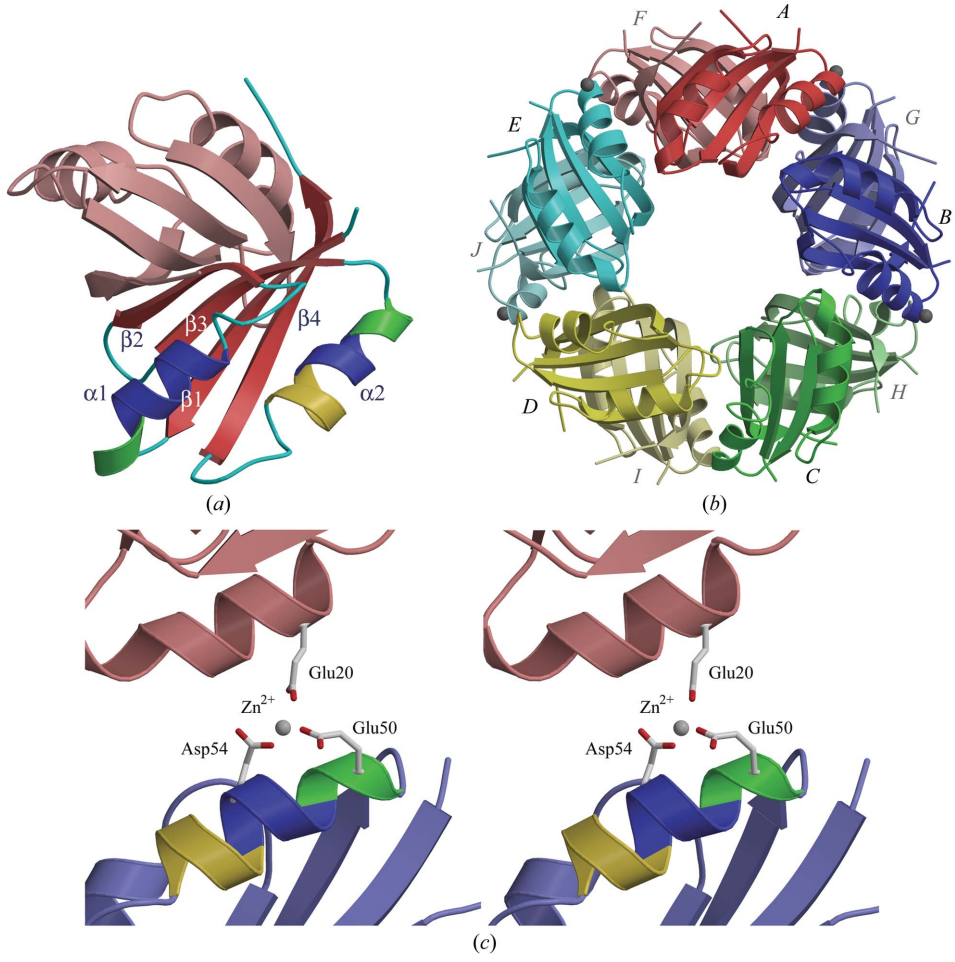

Figure 3
Schematic representation of the overall fold of the *T. thermophilus* SraA protein. (*a*) The dimeric structure (subunits *A* and *F*). The colour coding is the same as in Fig. 1. (*b*) The decameric structure. Subunits *A*–*J* are indicated. Zinc ions in the asymmetric unit are coloured grey. (*c*) Stereoview of the zinc-binding site. A zinc ion interacts with Glu50 and Asp54 of helix $\alpha2$ in subunit *B* and Glu20 of helix $\alpha1$ in subunit *A* of the neighbouring ring. These figures were prepared using *MOLSCRIPT* (Kraulis, 1991) and *RASTER3D* (Merritt & Murphy, 1994).

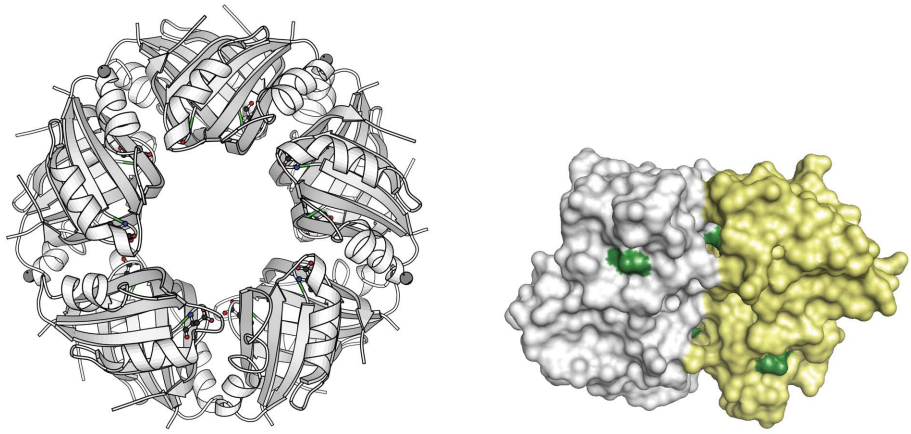

(*a*) (*b*)

Figure 4
(*a*) The Asp39 residues of SraA are coloured green on a ribbon diagram of the decameric ring. The side-chain atoms of Asp39 are represented by a ball-and-stick model. This figure was prepared with *MOLSCRIPT* (Kraulis, 1991). (*b*) The Asp39 residues are represented on the surface of the tetrameric SraA molecule composed of the *AF* (yellow) and *BG* (white) dimers. This figure was prepared using *PyMOL* (http://www.pymol.org).

interactions between the antiparallel β-sheets. In addition, the C-terminal β-strand (β4) interacts with the cleft formed by α1, β2 and β3 of another monomer and extends the β-sheet. The structure of the dimer is similar to those of the C-terminal RAM domains of *P. furiosus* LrpA and *Pyrococcus* sp. FL11 (Leonard *et al.*, 2001; Koike *et al.*, 2004) and the SARD protein *Pyrococcus* sp. DM1 (Koike *et al.*, 2003).

In the crystal lattice of the SraA protein, five dimers related by a non-crystallographic fivefold axis form a decamer in one asymmetric unit (Fig. 3*b*). This is consistent with the molecular weight of the protein being around 110 kDa in solution (Fig. 2*b*). The α2 helix and the loop connecting β3 and α2 are involved in hydrophobic interactions between two dimers, which form a ring composed of five dimers. The architecture of the α2 helix differs among the subunits (Fig. 3*b*). In subunits *A*, *B*, *E*, *G* and *I*, the α2 helix is composed of a 3_{10}-helix (three residues per turn, Val49–Glu51), an α-helix (four residues per turn, Leu52–Val55) and a π-helix (five residues per turn, Val56–Ile60). The 3_{10}-helix was not identified in subunits *D* and *F* and the π-helix was not identified in subunits *C* and *J*. In the case of subunit *H*, neither the 3_{10}-helix nor the π-helix was identified.

Four zinc ions exist on the external surface of the decameric ring (Fig. 3*b*). They interact with Glu50 and Asp54 of helix α2 in subunits *B*, *E*, *G* and *J* and coordinate with Glu20 of helix α1 in subunits *A*, *C*, *I* and *F* of the neighbouring ring in the crystal lattice, respectively (Fig. 3*c*). The 3_{10}-helix is necessary, but not sufficient, for zinc binding by the α2 helix. We found that the *B* factors of subunits *C*, *D*, *H* and *I* were higher (∼65 Å^2) than those of subunits *A*, *B*, *E*, *F*, *G* and *J* (∼45 Å^2). Subunits *C* and *D* form a dimer with subunits *H* and *I*, respectively, and none of these subunits bind a zinc ion at the α2 helices. The *B* factors of the zinc ion and the SraA protein were calculated to be ∼48 and ∼53 Å^2, respectively, when the occupancy of the zinc ion was assumed to be 1. These facts indicate that the zinc ions contribute to the stabilization of the crystal packing, which may be the reason why the SraA protein only crystallized in conditions containing zinc ions.

The external and internal diameters of the SraA ring are 70 and 20 Å, respectively. The size of the SraA ring is similar to the particle size of ∼65 Å for the octameric DM1 protein, as estimated by an electron-microscopic study (Clowney *et al.*, 2004).

The structure (subunit *A*) was compared with the structures in the Protein Data Bank (PDB) using the *DALI* program (Holm & Sander, 1998). The C-terminal RAM domains of *P. furiosus* LrpA and *Pyrococcus* sp. FL11 generated *Z* values of 13.4 and 13.2 and root-mean-square deviations of 1.5 and 1.2 Å, respectively. We could not compare the SraA structure with that of the *Pyrococcus* sp. DM1 protein because the coordinates have not been deposited in the PDB.

The structures of *P. furiosus* LrpA, *E. coli* AsnC, *B. subtilis* LrpC and *Pyrococcus* sp. DM1 (Leonard *et al.*, 2001; Koike *et al.*, 2003; Thaw *et al.*, 2006) revealed that the four dimers are arranged as a disc. In the structure of the *Pyrococcus* sp. FL11, the dimers form a sixfold helix, as also found with the RAM domains (Koike *et al.*, 2004). The structure of SraA, the SARD protein, is the first with a decameric RAM-domain ring.

The *P. furiosus* Q8U228 protein exhibited hydrolytic activity when *N*-CBZ-L-tyrosine *p*-nitrophenyl ester was used as a substrate (Agapay *et al.*, 2005). The protein was cocrystallized with 1,2-epoxy-3-(4-nitrophenoxy)propane, an aspartic protease inhibitor, and phenylmethylsulfonyl fluoride, a serine protease inhibitor. The Q8U228 protein contains one serine residue, Ser70, which is not conserved in the SraA protein. Interestingly, a *BLAST* search revealed that Asp39 of SraA, corresponding to Asp39 of Q8U228, was identical among 43 bacterial and 17 archaeal SARD proteins (data not shown). This residue is located at the dimer–dimer interface of the internal surface of the decameric ring (Fig. 4). A cleft exists close to Asp39 and the substrate might pass through it (Fig. 4*b*). Thus, Asp39 might be one of the catalytic residues of SraA. We did not detect any hydrolytic activity when SraA was incubated with the same substrate as that used with the Q8U228 protein (data not shown). Therefore, the substrate specificity might differ between the SraA and Q8U228 proteins.

This work was supported by the RIKEN Structural Genomic/Proteomics Initiative (RSGI), the National Project on Protein Structural and Functional Analyses, Ministry of Education, Culture, Sports, Science and Technology of Japan.

References

Agapay, R. C., Savvides, S. N., Van Driessche, G., Devreese, B., Van Beeumen, J., Jongejan, J. A. & Hagen, W. R. (2005). *Acta Cryst.* F**61**, 914–916.
Bell, S. D. & Jackson, S. P. (2001). *Curr. Opin. Microbiol.* **4**, 208–213.
Brinkman, A. B., Ettema, T. J., de Vos, W. M. & van der Oost, J. (2003). *Mol. Microbiol.* **48**, 287–294.
Brünger, A. T., Adams, P. D., Clore, G. M., DeLano, W. L., Gros, P., Grosse-Kunstleve, R. W., Jiang, J.-S., Kuszewski, J., Nilges, M., Pannu, N. S., Read,

R. J., Rice, L. M., Simonson, T. & Warren, G. L. (1998). *Acta Cryst.* D**54**, 905–921.
Calvo, J. M. & Matthews, R. G. (1994). *Microbiol. Rev.* **58**, 466–490.
Clowney, L., Ishijima, S. A. & Suzuki, M. (2004). *Proc. Jpn Acad. B*, **80**, 148–155.
Emsley, P. & Cowtan, K. (2004). *Acta Cryst.* D**60**, 2126–2132.
Ettema, T. J., Brinkman, A. B., Tani, T. H., Rafferty, J. B. & van der Oost, J. (2002). *J. Biol. Chem.* **277**, 37464–37468.
Geiduschek, E. P. & Ouhammouch, M. (2005). *Mol. Microbiol.* **56**, 1397–1407.
Holm, L. & Sander, C. (1998). *Nucleic Acids Res.* **26**, 316–319.
Kabsch, W. & Sander, C. (1983). *Biopolymers*, **22**, 2577–2637.
Koike, H., Ishijima, S. A., Clowney, L. & Suzuki, M. (2004). *Proc. Natl Acad. Sci. USA*, **101**, 2840–2845.
Koike, H., Sakuma, M., Mikami, A., Amano, N. & Suzuki, M. (2003). *Proc. Jpn Acad. B*, **79**, 63–69.
Kraulis, P. J. (1991). *J. Appl. Cryst.* **24**, 946–950.
Kudo, N., Allen, M. D., Koike, H., Katsuya, Y. & Suzuki, M. (2001). *Acta Cryst.* D**57**, 469–471.
Kuramitsu, S., Hiromi, K., Hayashi, H., Morino, Y. & Kagamiyama, H. (1990). *Biochemistry*, **29**, 5469–5476.
Laemmli, U. K. (1970). *Nature (London)*, **227**, 680–685.
Laskowski, R. A., MacArthur, M. W., Moss, D. S. & Thornton, J. M. (1993). *J. Appl. Cryst.* **26**, 283–291.
Leonard, P. M., Smits, S. H., Sedelnikova, S. E., Brinkman, A. B., de Vos, W. M., van der Oost, J., Rice, D. W. & Rafferty, J. B. (2001). *EMBO J.* **20**, 990–997.
Mendel, S., Elkayam, T., Sella, C., Vinogradov, V., Vyazmensky, M., Chipman, D. M. & Barak, Z. (2001). *J. Mol. Biol.* **307**, 465–477.
Merritt, E. A. & Murphy, M. E. P. (1994). *Acta Cryst.* D**50**, 869–873.
Morris, R. J., Perrakis, A. & Lamzin, V. S. (2003). *Methods Enzymol.* **374**, 229–244.
Murshudov, G. N., Vagin, A. A. & Dodson, E. J. (1997). *Acta Cryst.* D**53**, 240–255.
Newman, E. B. & Lin, R. (1995). *Annu. Rev. Microbiol.* **49**, 747–775.
Otwinowski, Z. & Minor, W. (1997). *Methods Enzymol.* **276**, 307–326.
Ouhammouch, M. (2004). *Curr. Opin. Genet. Dev.* **14**, 133–138.
Sakuma, M., Koike, H. & Suzuki, M. (2005). *Proc. Jpn Acad. B*, **81**, 26–32.
Schuller, D. J., Grant, G. A. & Banaszak, L. J. (1995). *Nature Struct. Biol.* **2**, 69–76.
Suzuki, M. (2003). *Proc. Jpn Acad. B*, **79**, 274–289.
Terwilliger, T. C. (2001). *Acta Cryst.* D**57**, 1763–1775.
Terwilliger, T. C. & Berendzen, J. (1999). *Acta Cryst.* D**55**, 849–861.
Thaw, P., Sedelnikova, S. E., Muranova, T., Wiese, S., Ayora, S., Alonso, J. C., Brinkman, A. B., Akerboom, J., van der Oost, J. & Rafferty, J. B. (2006). *Nucleic Acids Res.* **34**, 1439–1449.
Thompson, J. D., Higgins, D. G. & Gibson, T. J. (1994). *Nucleic Acids Res.* **22**, 4673–4680.
Yokoyama, K., Ishijima, S. A., Clowney, L., Koike, H., Aramaki, H., Tanaka, C., Makino, K. & Suzuki, M. (2006). *FEMS Microbiol. Rev.* **30**, 89–108.